

Influence of Compatibilizer on Notched Impact Strength and Fractography of HDPE–Organoclay Composites

Waraporn Rattanawijan,¹ Tawechai Amornsakchai,^{1,2} Pornsawan Amornsakchai,³
Pinsupha Petiraksakul⁴

¹Department of Chemistry and Center of Excellence for Innovation in Chemistry, Faculty of Science, Mahidol University, Salaya, Nakhonpathom 73170, Thailand

²Center for Alternative Energy, Faculty of Science, Mahidol University, Salaya, Nakhonpathom 73170, Thailand

³Department of Chemistry, Faculty of Science, Naresuan University, Phitsanulok 65000, Thailand

⁴Department of Materials Technology, Faculty of Science, Ramkhamhaeng University, Huamark, Bangkok, Bangkok 10240, Thailand

Received 6 July 2008; accepted 27 January 2009

DOI 10.1002/app.30181

Published online 17 April 2009 in Wiley InterScience (www.interscience.wiley.com).

ABSTRACT: The focus of this study was the notched impact property of high-density polyethylene (HDPE)–organoclay composites and the resultant morphology of impact-fractured surfaces. Composites with a different organoclay content and degree of organoclay dispersion were compared with neat HDPE under identical conditions. The degree of organoclay dispersion was controlled through the use of a compatibilizer, maleic anhydride grafted polyethylene. It was found that the addition of organoclay can slightly increase the elastic modulus and notched impact strength of the composite. When the level of organoclay dispersion was improved by using compati-

bilizer, elastic modulus and toughness further increased. A significant increase in yield strength was also notable. The presence of organoclay was found to suppress strain hardening of the matrix during tensile testing. The impact-fractured surfaces of failed specimens were studied with scanning electron microscopy. The micromechanism for the increased toughness of HDPE–organoclay composites was discussed. © 2009 Wiley Periodicals, Inc. *J Appl Polym Sci* 113: 1887–1897, 2009

Key words: polyethylene composites; organoclay; impact property; fractography

INTRODUCTION

High-density polyethylene (HDPE) is one of the important semicrystalline polymeric materials that is widely used because of its low costs and ease of processing.¹ HDPE, as other polymers, is frequently used in mineral-filled forms to reduce the cost of the polymer and to modify mechanical properties, especially modulus.² There are also other advantages such as improved heat distortion temperature and better mold shrinkage.³ In recent years, there has been a great deal of interests in nanocomposites from HDPE and other low-cost commodity polymers. One of the reinforcements that is widely used in polymer nanocomposites is organically modified layered silicates or organoclay. Since organoclay pri-

mary platelets have a very large aspect ratio, it is expected that a significant level of improvement in mechanical property may be obtained with low organoclay loading (typically less than 5 wt %).⁴ However, the effect of organoclay on tensile properties varies from polymer to polymer. For nylon, the improvement in modulus can be as high as 200% due to the strong polar–polar interaction.^{5,6} For non-polar polymers such as polyethylene or polypropylene, the level of improvement is much lesser and varies, depending on the level of degree of dispersion.^{7–10} Another important mechanical property that could determine the application of a material is impact strength. HDPE is generally known to be quite tough at normal temperatures and moderate rates of deformation. It is, however, notch-brittle at low temperatures and under impact loading.¹¹ The addition of mineral fillers will generally have embrittling effects by sharply decreasing the polymer impact energy. Similarly, HDPE nanocomposites also have poor impact strength due to the present of rigid particles. It is clear that there is a need for HDPE with high modulus and high impact strength.

Most studies of modification using rigid particulate fillers report a significant decrease in toughness compared with neat polymers. An increase in

Correspondence to: T. Amornsakchai (sctam@mahidol.ac.th).

Contract grant sponsor: Thailand Research Fund; contract grant number: RSA4580038.

Contract grant sponsor: Center for Innovation in Chemistry: Postgraduate Education and Research Program in Chemistry (PERCH-CIC), Commission on Higher Education, Ministry of Education.

toughness has been reported in filled polypropylene^{2,12} and filled polyethylene.^{2,13–18} An impressive increase of impact energy by a factor of nearly 4 was reported by Wang and coworkers^{15–19} for polyethylene filled with calcium carbonate particles. Toughenability has been correlated with the critical interparticle ligament dimension^{20,21} and was later shown to be due to preferred orientation around the calcium carbonate particles²² and small spherulite size and the amorphous nature of the polymer matrix–particle interface.²³ The extent of improvement of mechanical properties of mineral-filled polymer composites depends on the structure and aspect ratio of the filler. Particulate fillers that can improve toughness should have an average aspect ratio close to unity, to minimize the matrix ligament thickness according to Wu's criterion.^{20,21} Those characterized by a layered structure, such as clay,^{24,25} or high aspect ratio, wollastonite,²⁶ are not preferred from the viewpoint of toughness. The reported impact strength of HDPE–organoclay nanocomposites varies widely. It may be significantly dropped,²⁷ slightly dropped,⁹ maintained,⁹ or even slightly improved over that of the base polymer.⁹ Despite a number of reports, there is still discrepancy among published literature regarding the toughening of HDPE with a rigid filler of a different shape. It is therefore obvious that more studies are needed to gain a better understanding of the effect of high aspect ratio filler on the impact failure mechanism. In this study, the focus is on the effect of organoclay and compatibilizer content on tensile and impact properties. The morphology of fractured surfaces was investigated to understand the changes in failure mechanism.

EXPERIMENTAL

Materials

HDPE with an MFI of 4 g/10 min grade Thai-Zex 2208 J produced by Bangkok Polyethylene (Rayong, Thailand), was used. Organoclay, which is commercially available under the trade name Claytone[®] HY, produced by Southern Clay Products (Gonzales, TX), was purchased from a local distributor. According to product literature, the clay is organically modified montmorillonite (OMMT). Commercial maleic anhydride grafted high-density polyethylene (PE-*g*-MA), known as Fusabond[®] E series grade MB 100D (Samia, Canada), was used as a compatibilizer. It has about 1% maleic anhydride content and a density of 0.96 g/cm³; MFI is 2 g/10 min.

Preparation of HDPE–organoclay composites

The HDPE–organoclay composites were prepared by melt-blending with a laboratory two-roll mill at 150–

TABLE I
Sample Designations and Compositions

Sample designation	Composition (parts)		
	HDPE2208	Organoclay	Compatibilizer
PE08	100	–	–
PE08OM3	100	3	–
PE08OM5	100	5	–
PE08OM7	100	7	–
PE08OM7CP3.5	96.5	7	3.5
PE08OM7CP7	93	7	7
PE08OM7CP14	86	7	14

155°C. The HDPE was melted on the mill first and then a predetermined amount of organoclay was added and mixing continued until no lumps of organoclay were observed. Organoclay can be easily incorporated into molten HDPE. An opaque pale yellowish composite was obtained. The amount of organoclay in the composites were 3, 5, and 7 wt % of HDPE (phr). To study the effect of the compatibilizer, composite with 7 phr organoclay was chosen and compatibilizer was added at 3.5, 7, and 14 wt % of the total polymer. The composites were ground with a granulator and then pelletized with a twin screw extruder. The twin screw extruder temperature profile was 135, 150, 160, 160, and 165°C from hopper to die, and the screw speed was 150 rpm. The sample codes were PE08, PE08OM x , and PE08OM7CP y for neat HDPE and composites. For the latter, x and y represent the amount of organoclay and compatibilizer, respectively. Sample designations and compositions are shown in Table I.

X-ray characterization

Measurements of state of dispersion and the interlayer spacing of the organoclay in the composites were carried out on a Bruker AXS D8 X-ray diffractometer. A sample size of 30 mm × 30 mm was cut from a 1-mm-thick compressed sheet and placed in the sample holder of X-ray diffractometer. The plane of incident X-ray always made angle θ with the sample surface. The scanning angle for all the experiments was between $2\theta = 1.5$ – 10° and step size of 0.015° . The X-ray generator was operated at 40 kV and 30 mA.

Injection molding of HDPE–organoclay composites

The composite was converted into specimens for tensile and impact tests with an injection molding machine. The processing temperatures were 180, 190, and 200°C from hopper to nozzle, and the mold temperature was around 40°C. The mold contained three cavities. One was a tensile specimen and the others were rectangular specimens for impact and

flexural tests. The dimensions of these specimens are described in the following related sections. Flow or machine direction was parallel to the longitudinal direction of the injected specimens.

Tensile testing

The tensile specimens were type IV. The width of the narrow section was 6 mm; the length of the narrow section is 33 mm. The distance between the grips was 25 mm and the cross-head speed was 50 mm/min, in accordance with ASTM D638. The test was conducted at room temperature with an Instron universal tester (Model 5566). Strain was calculated from grip separation divided with an initial gauge length of 25 mm. Secant modulus at 1% strain and tensile yield strength were calculated for each specimen. The yield strength is the maximum in the stress-strain curve just beyond the elastic region. An average of 10 measurements for each composite composition were taken.

Impact testing

Injected specimens were 62 mm (length) \times 12 mm (width) \times 3.3 mm (thickness). The samples were notched with a Davenport notch cutting apparatus to a depth of about 1.3 mm. Notched Izod impact strength was measured with a Radmana ITR-2000 instrumented impact tester (McVan Instruments, Australia). The test was performed at room temperature with the impact velocity of 3.5 m/s. An average of 10 measurements for each composite composition was reported. Failed specimens were collected for subsequent observation under an electron microscope.

Differential scanning calorimetry

The crystallinity of neat HDPE and composites was measured on small samples cut from injected tensile bars. The measurement was carried out using a Perkin-Elmer instrument (differential scanning calorimetry, DSC-7). The instrument was calibrated using high purity Indium and Zinc. The samples were scanned at temperatures between 50 and 180°C at a heating rate of 20°C/min. All data from the composites were normalized to account for organoclay content. PE crystallinity values were determined from heat of fusion data, assuming the heat of fusion of a 100% crystalline polyethylene to be 293 J/g.²⁸

Scanning electron microscopy

To observe the internal morphology, the sample surface was removed at a low temperature with a glass knife in microtome. The exposed surface was etched with a permanganic reagent²⁹ for 1 h at room tem-

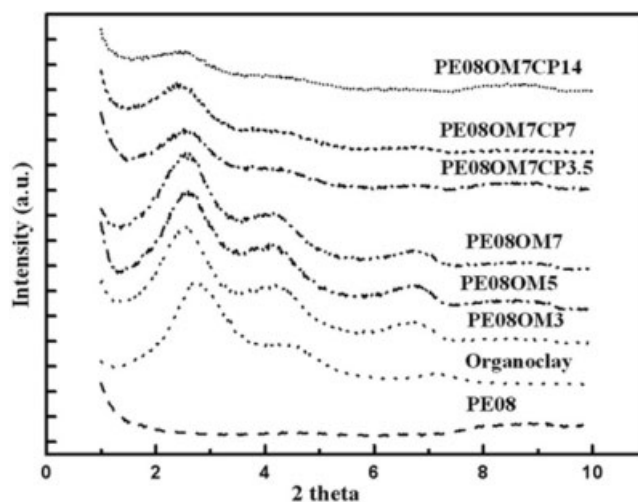


Figure 1 X-ray diffraction patterns of PE08, organoclay, and composites.

perature. Etched specimens and impact-fractured specimens were then gold coated. Surface morphology of these specimens was observed with a Leo model 1455 VP scanning electron microscope (SEM) operating at 5.00 kV with no specimen tilt.

RESULTS AND DISCUSSION

XRD

XRD patterns provide useful information of the gallery size of organoclay in the composite. Figure 1 shows the XRD patterns of neat HDPE (PE08), organoclay, and HDPE composites containing different amounts of organoclay and compatibilizer. The PE08 does not show any scattering peak in the region studied, whereas the organoclay shows a few peaks, with the strongest at around 2.8°. For the HDPE composites, the organoclay peak shifted slightly to a lower scattering angle. The peak appears to remain at around 2.56° for HDPE composites containing 3, 5, and 7 phr organoclay. The shift to a lower angle indicates that the organoclay gallery is wider and would suggest an intercalated structure. It is also shown in Figure 1 that when a compatibilizer was added in to the system, the peak shifted further to a lower angle. The peak also became wider, and its intensity decreased significantly. This would suggest that a better intercalation and breakdown of organoclay particles were obtained. The degree of organoclay dispersion in compatibilized HDPE composites was better than in the uncompatibilized composites. This is a result of the strong interaction between polar PE-g-MA molecules and the organoclay. Therefore PE-g-MA can penetrate the galleries of the organoclay easily. The change in dispersion of organoclay will become clearer when morphology of the composites is considered in the following section.

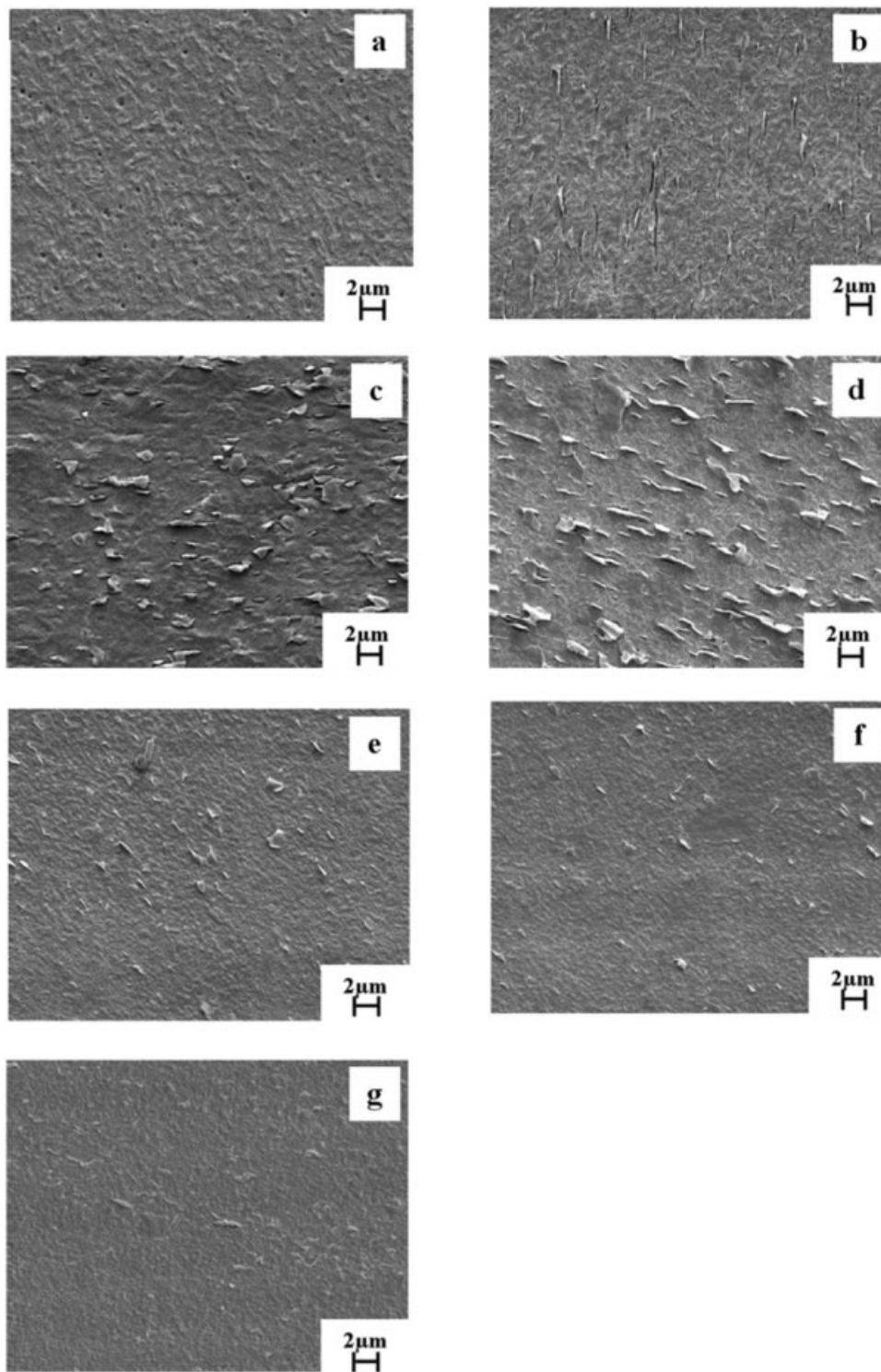


Figure 2 SEM micrographs of etched surface showing internal morphology of PE08 and composites containing different organoclay and compatibilizer content. (a) PE08, (b) PE08OM3, (c) PE08OM5, (d) PE08OM7, (e) PE08OM7CP3.5, (f) PE08OM7CP7, and (g) PE08OM7CP14.

Internal morphology

Figure 2 shows the etched surfaces of PE08 and composites with different organoclay and compatibilizer content. PE08 displays a fine crystalline texture. For composites containing 3, 5, and 7 phr

organoclay, organoclay platelets can still be seen. The dispersion of the organoclay is quite uniform, and the number of organoclay platelets or tactoids increase with increasing organoclay content. The size of organoclay tactoids appears to be thicker

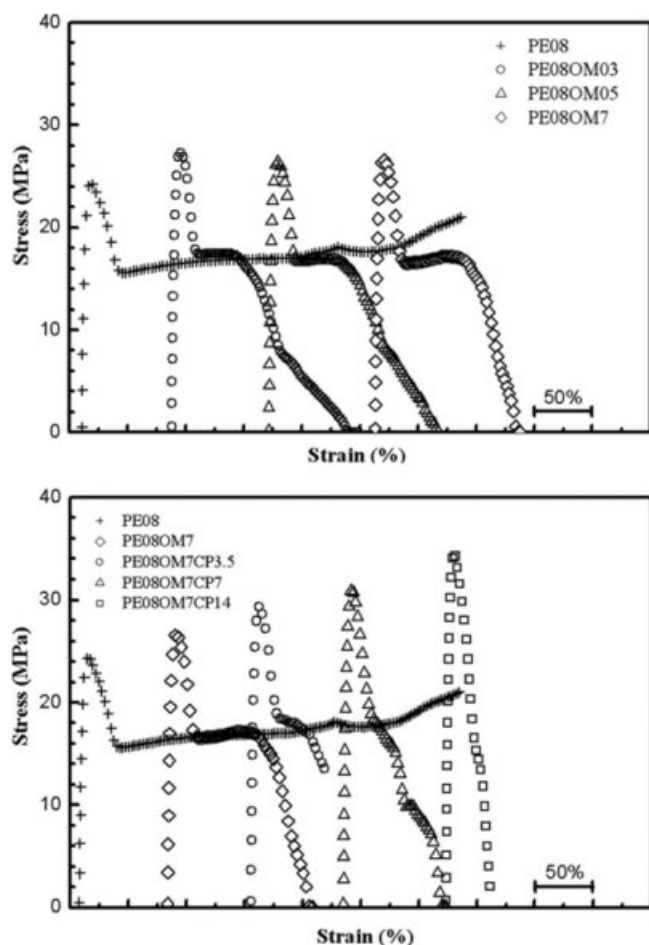


Figure 3 Stress-strain curves of PE08 and composites containing different organoclay content (top) and PE08, PE08OM7, and composites with different compatibilizer content (bottom).

with increasing organoclay content. When a compatibilizer was added, the size of the organoclay tactoids became much smaller. Large tactoids can still be seen, and the number of these large tactoids decreased with increasing compatibilizer content. At the highest compatibilizer content, no large tactoid could be seen. These results confirm that the compatibilizer can help improve the degree of organoclay

dispersion significantly, and this is consistent with the XRD results shown previously.

Tensile properties

Under tensile deformation, PE08 exhibits cold drawing behavior (Fig. 3). Upon tensile deformation, stress increases and then drops when necks are formed. The necks then propagate outward while the stress remains relatively constant. When the necks reach both ends of the specimen, the specimen is completely drawn. Further deformation will result in an increase in stress due to the orientation in the specimen. The addition of organoclay appears to reduce the cold drawability. When necks were formed in the composites, the necked part was not stable. It became thinner, as seen from the load drop, as deformation progressed. Finally, the composites failed. For compatibilized composites, the cold drawability decreased even further. At the highest compatibilizer content (PE08OM7CP14), the specimen thinned down right away after the necks were formed. This clearly indicated a significant reduction in resistance to plastic deformation. Since the area under tensile stress-strain curve can be used to indicate the toughness of the specimen, it may be concluded that at this rate of (tensile) deformation, the composites, both uncompatibilized and compatibilized, lost their toughness.

From the stress-strain curves shown in Figure 3, modulus and yield strength of PE08 and composites can be calculated. These are tabulated in Table II. It can be seen that modulus increased slightly with the addition of organoclay, whereas yield strength increased and then dropped slightly. Modulus and yield strength further increased with the addition of a compatibilizer. The highest improvement was observed in PE08OM7CP14, which contained the highest organoclay and compatibilizer contents in this study. The levels of improvement for modulus and yield strength were about 36 and 44%, respectively. This is comparable to that observed in other polyolefin systems⁷⁻¹⁰ but significantly higher than

TABLE II
Yield Strength, Modulus, Melting Temperature, and Crystallinity of Neat HDPE and HDPE-Organoclay Composites

Samples	Yield strength (MPa)	Modulus at 1% strain (MPa)	Peak melting temp. (°C)	Normalized crystallinity (%)
PE08	25.4 ± 1.2	1035 ± 25	133	67
PE08OM3	27.4 ± 0.2	1144 ± 33	132	59
PE08OM5	26.7 ± 0.2	1163 ± 7	132	59
PE08OM7	26.5 ± 0.6	1173 ± 29	133	61
PE08OM7CP3.5	29.7 ± 0.3	1267 ± 33	133	60
PE08OM7CP7	30.4 ± 0.6	1285 ± 28	133	61
PE08OM7CP14	34.5 ± 0.3	1493 ± 45	133	64

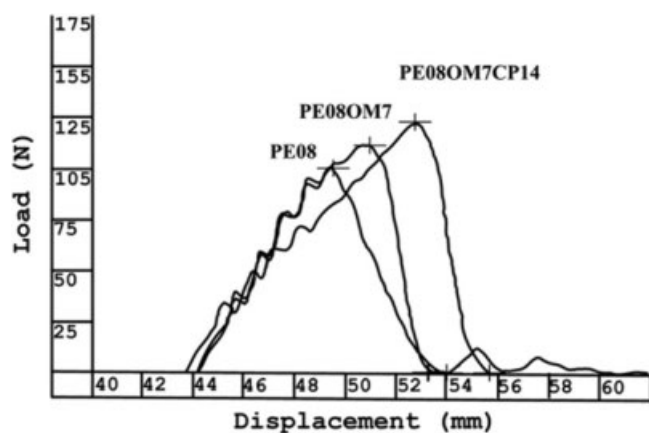


Figure 4 Load–displacement curves from instrumented impact test for PE08, PE08OM7, and PE08OM7CP14.

that of particulate-filled HDPE.^{13,23} This illustrates clearly the benefit of organoclay over conventional particulate filler.

It is generally known that modulus and yield strength of HDPE depends on crystallinity.³⁰ However, melting enthalpy of PE08 and composites measured with a DSC showed that composites have slightly lower crystallinity than PE08 without a specific trend as shown in Table II. Therefore, the observed changes in the tensile properties cannot be due to a change in crystallinity and is more likely to be due to the presence of the highly anisotropic organoclay platelets. This is in line with the findings reported elsewhere.^{10,31} Therefore, the monotonous increase in the yield stress with increased compatibilizer content would suggest the increasing exfoliation and also a stronger attraction between organoclay and the HDPE matrix (through the use of PE-g-MA compatibilizer).

It has been shown that the modulus of the polymer–clay composite can be predicted with the well-established Christensen's equation and the derivatives of Hashin-Shtrikman bounds employed in conventional composites.³² Our data are too limited for a modeling of the modulus of the composites. However, if we take our best sample, PE08OM7CP14, and assume that the degree of dispersion in our sys-

tem is comparable to that in,³² the enhancement in the modulus, in terms of composite modulus (E_c) to polymer modulus (E_p) ratio in our system, is greater than that found in³² ($E_c/E_p \approx 1.44$ as compared with 1.2). Perhaps the organoclay platelets in our system were not randomly oriented as in Ref. 32 but had a certain degree of orientation due to the injection moulding process.³²

Impact property

The instrumented falling weight impact tester was used to determine notched impact strength of PE08 and composites. The load–displacement curve was recorded for each specimen. Generally, a typical load–displacement curve, as shown in Figure 4, can be divided into two regions, i.e., fracture initiation energy and propagation energy. The former is defined as the sum of the energy absorbed until maximum load, and the latter is the energy absorbed after the maximum load. The sum of the two is total impact energy. The load–displacement curves of PE08 and selected composites are shown in Figure 4, and the corresponding average impact energies of all samples are tabulated in Table III. Clearly, the addition of organoclay increased the impact property of the composites but the organoclay content had little effect on the impact energy. When a compatibilizer is added, there is improvement. Again, the compatibilizer content does not affect the impact energy. The increase in impact energy for the composites appeared to be dominated by the fracture initiation energy and can be seen when comparing the load–displacement curves shown in Figure 4. The increase in fracture initiation energy could be attributed to the changes in mechanical properties and resistance to plastic deformation of the composites shown earlier.

From the results shown above, it is clear that at the deformation rate of impact test our HDPE–organoclay composites is tougher than PE08. The apparent increases in impact strength depend on the degree of organoclay dispersion. It is worth pointing out that the impact strength of HDPE–organoclay

TABLE III
Impact Energy of PE08 and Composites Containing Different Organoclay and Compatibilizer Content

Samples	Fracture initiation energy, E_i (kJ/m ²)	Fracture propagation energy, E_p (kJ/m ²)	Impact strength σ_i (kJ/m ²)
PE08	14.9 ± 3.8	5.7 ± 1.3	20.6 ± 4.0
PE08OM3	19.4 ± 6.0	3.8 ± 1.1	23.3 ± 5.4
PE08OM5	17.3 ± 5.4	5.2 ± 5.6	22.4 ± 4.5
PE08OM7	19.6 ± 3.8	3.5 ± 0.4	23.1 ± 3.6
PE08OM7CP3.5	24.5 ± 5.5	3.7 ± 0.4	28.2 ± 5.7
PE08OM7CP7	23.3 ± 5.1	4.6 ± 3.9	27.9 ± 1.7
PE08OM7CP14	26.7 ± 1.5	3.5 ± 0.4	29.3 ± 1.8

reported in literature is rather limited and varies. Zhao et al.⁹ studied uncompatibilized HDPE-organoclay composites and found that the impact strength dropped, depending on the type of intercalating agent employed and the organoclay content. Only in one case was a 10% increase in impact strength observed, and then the impact strength dropped with increased organoclay content. It has also been suggested that the layered structure, such as clay,^{24,25} or a high aspect ratio, wollastonite,²⁶ are not preferred for toughness improvement. However, we observed an increase of 42% in toughness.

The reason that a large increase in toughness was observed could be due to the HDPE matrix employed. We used an injection molding grade that has a lower molecular weight than the blow molding grade used by Tanniru et al.²⁷ The impact strength of HDPE is known to depend on molecular weight, and the impact strength increases with increasing molecular weight.³⁰ A filler would have a deteriorating effect in high molecular weight HDPE. In addition, it could also be due to the type of organoclay and the use of a compatibilizer, which promoted a greater dispersion of organoclay platelets in our case. Work is now underway to get a better understanding of the effect of these factors.

The impact load-displacement curve for HDPE and its composites display a relatively sharp drop after the peak (Fig. 4), indicating limited macroscopic yielding of the materials occurred during crack propagation. It is therefore proposed that the mechanism that operates in our system may be different from that which operates in other rigid particulate-filled systems.^{11,15-19,23,33} The presence of organoclay platelets, especially in the compatibilized systems, appears to reduce notch sensitivity of the material and allows it to deform to larger strain before crack propagation takes place.

Impact fractured surfaces

The structure or morphology of a fractured surface can provide useful information regarding the nature of failure. This can help to better understand the change in the impact strength of the composites. Figure 5 shows a typical macroscopic structure with parabolic morphology of the impact fractured surface of PE08. This parabolic morphology is a result of the so-called stick-slip process.³⁴ Highly magnified images of different regions are shown in Figure 5(a-f). The rather flat region next to the notch [Fig. 5(a)] shows a craze-like region with large vein-type features involving the tearing of the material.³⁵ Ahead of region (a) is a stick-slip region shown under high magnification in Figure 5(b). In the "stick" region [Fig. 5(c)], much drawing or plastic deformation occurs. Conversely, in the "slip" region

[Fig. 5(d)], much less of such a process is evident. Such phenomena lead to a stop-go action of the crack front,³⁶ resulting in a large energy absorption. The stick-slip process is accompanied by stress relaxation. Stick-slip or stop-go propagation, associated with the dynamic crack propagation effects, occurs when the speed of the crack is below a critical value. At this point, the crack stops or arrests (sticks). When the stress increases or builds up again, the crack re-initiates and propagates (slips).³⁷ A high magnification image of a stick region is shown in Figure 5(c). An extensive drawing of fibrils can be seen. This slip region shows shallow vein-type features. The shear slip areas at the top and bottom of the macroscopic image are shown in Figure 5(e). In this region, striations or fibrils can be seen.³⁵ The plastic deformation zones are perpendicular to the local crack growth. On the far left is a plastic deformation zone that parallels the crack growth [Fig. 5(f)]. It should be noted that our impact-fractured surface of neat HDPE (PE08) is very similar to that reported by Ravi and Takahashi³⁴ but is very different from that reported by Tanniru and Misra²³ and Tanniru et al.²⁷ The difference in fracture morphology in the latter case is due mainly to the molecular weight of HDPE employed as discussed earlier. However, local or microscopic morphologies are similar and comparable.

In contrast to PE08, the impact-fractured surfaces of all HDPE-organoclay composites display a brittle-like appearance at the macroscopic level. No stick-slip can be seen. Figure 6 displays the macroscopic fractured surfaces of PE08OM3, PE08OM5, and PE08OM7. There are no significant differences in appearance among the composites with different amounts of organoclay except that there appears to be a transition in morphology [Fig. 6(b)]. Fractured surfaces can be divided into two to three regions, according to the microscopic morphology. For the largest region (A), starting just after the notch, it appears to be covered with microvoids and with ligaments linked between the microvoids [Fig. 6(d)]. Organoclay platelets can be seen in the cavities, inside the circle. The remaining region (B, C), at the end of the fractured surface, displays plastic deformation or fibrillation zone as seen in PE08 [Fig. 5(f)]. The morphology of this region appears to change with organoclay content. At low organoclay content, PE08OM3 shows fibrillation with undulation [Fig. 6(a)]. PE08OM5 [Fig. 6(b)] illustrates fibrillation with undulation in part of the region and without undulation in the rest. At high organoclay content, PE08OM7, the morphology changes to fibrillation without undulation [Fig. 6(c)]. Fibrillation with or without undulation as seen here is similar to layered and nonlayered fibrillation reported by Tanniru and Misra³⁸ in calcium carbonate-filled HDPE. The cause

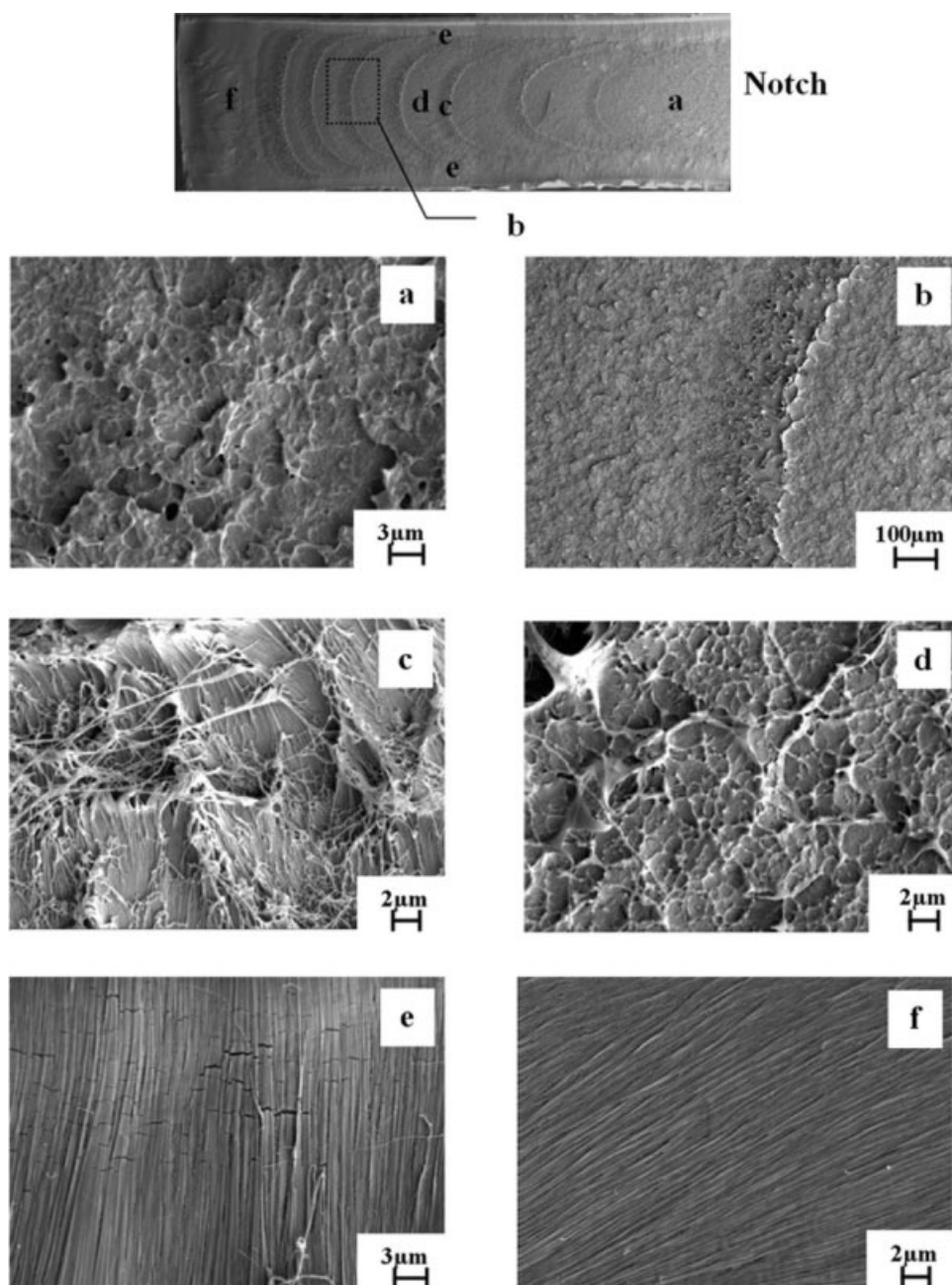


Figure 5 SEM micrographs showing macroscopic view of impact fractured surface of PE08. High magnification images of different regions labeled (a–f) are also shown.

of such morphology has been given.³⁸ This suggests that as the level of organoclay content increases, the microscopic morphology of the final region changes from layered to nonlayered fibrillation. However, this change has little effect on the impact strength of the composite.

The macroscopic fractured surfaces of compatibilized HDPE composites also display a brittle-like appearance, and that of PE08OM7CP7 is presented as an example in Figure 7. There are no significant differences in appearance among the composites with differing amounts of compatibilizer. The frac-

tured surface seems to have two zones with different macroscopic morphology. Under high magnification, microscopic morphology of the two zones is not distinguishable. High-magnification views of the morphology of PE08OM7CP3.5, PE08OM7CP7, and PE08OM7CP14 are presented in Figure 7(a–c, respectively). The morphology seen is similar to that of the uncompatibilized composites [Fig. 6(d)] but the size of microvoid is much smaller for the compatibilized composites. It is easier to visualize in terms of number of cavities per area. To obtain this value, a rectangle of arbitrary size was drawn in enlarged SEM

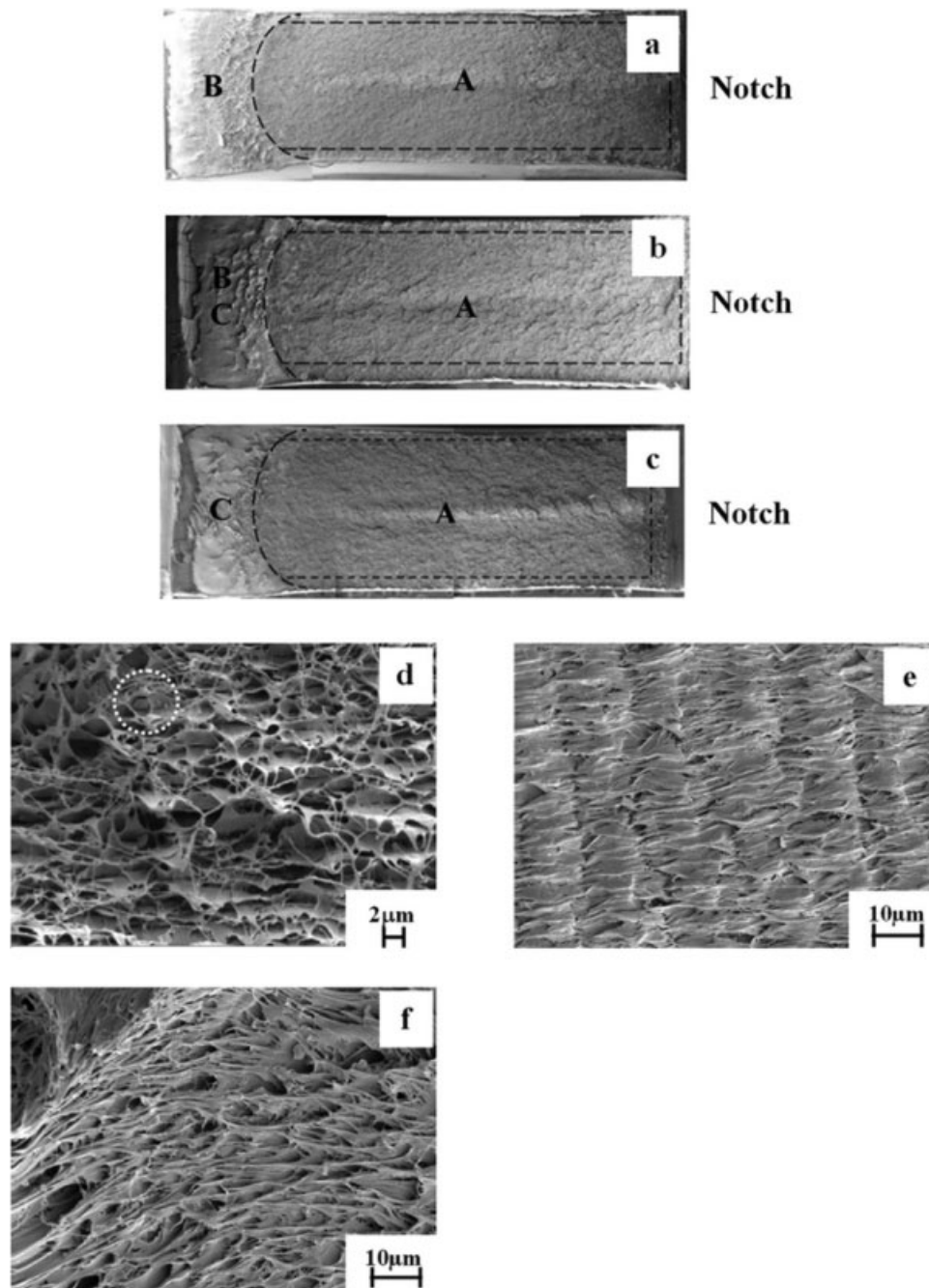


Figure 6 SEM micrographs showing macroscopic view of impact-fractured surface of (a) PE08OM3, (b) PE08OM5, and (c) PE08OM7. High magnification images of different regions labeled A, B, and C are shown in (d), (e), and (f), respectively. Image (d) was taken from PE08OM3 and images (e) and (f) were from PE08OM5.

images of the corresponding samples and the number of cavities was counted manually with the aid of ImageTool software.³⁹ The value for uncompatibilized composites is in the order of 20–40 cavities per $100 \mu\text{m}^2$, whereas that for compatibilized composites is in the order of 200–300 cavities per $100 \mu\text{m}^2$. The large number of cavities reflect the large number of nucleation sites for microvoiding. A large number of nucleation sites per area will consequently limit the size of microvoids.

Haworth et al.⁴⁰ have shown that high dispersion and low particle–polymer interaction are fundamental to the development of matrix yielding and plastic deformation adjacent to the filler particles. This represents the origin of the enhanced impact resistance observed in mineral-filled medium-density polyethylene and was confirmed by fractographic analysis. A similar mechanism is likely to occur in our system, in which failure initiation mechanism changes to nucleation of microvoids was a result of the

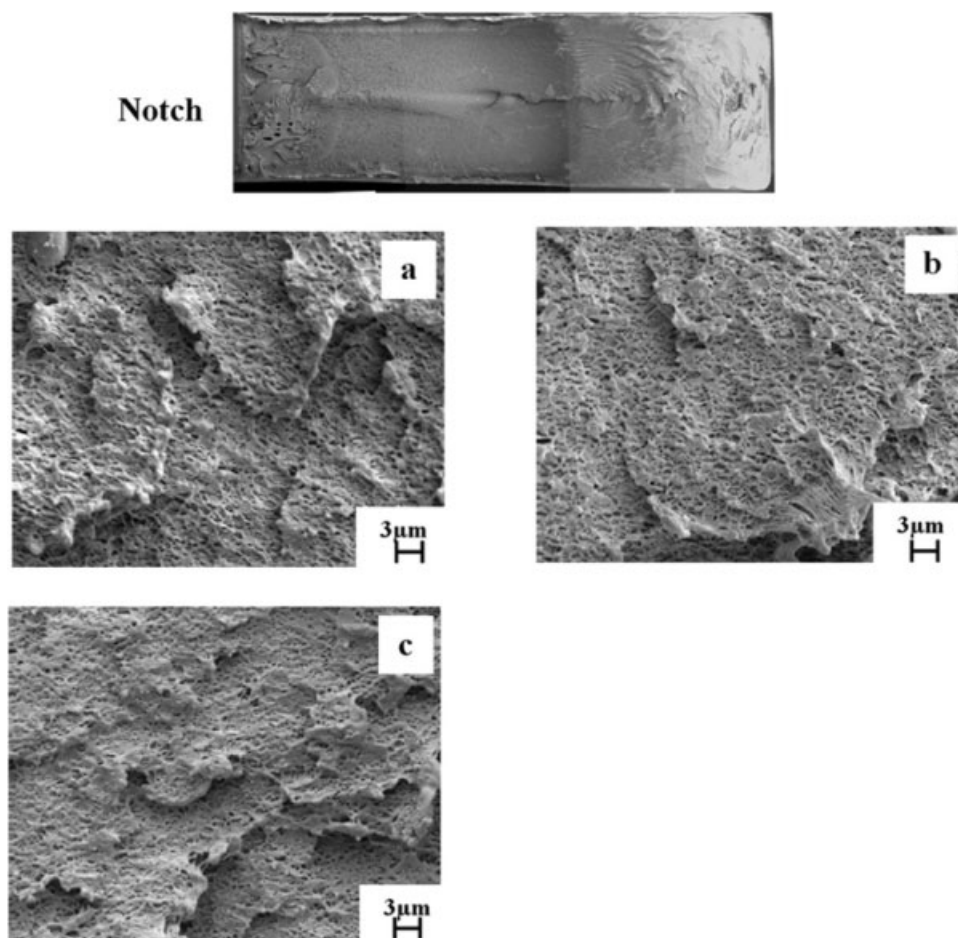


Figure 7 SEM micrographs showing macroscopic view of impact-fractured surface of PE08OM7CP3.5. High magnification images of representative area of each compatibilizer content are shown. (a) PE08OM7CP3.5, (b) PE08OM7CP7, and (c) PE08OM7CP14.

interfacial failure between organoclay and the surrounding matrix. In PE08OMx, the size of organoclay platelets is quite large [Fig. 2(b–d)]. The presence of organoclay platelets in PE08OMx would cause stress concentration around the platelets. The matrix yielding and plastic deformation adjacent to the filler particles then developed. Composites with compatibilizer (PE08OM8CPy) display improved yield strength (Table II). They will, therefore, require more energy to cause yielding. Since interfacial failure and yielding processes have been suggested to occur in the initiation stage of impact failure,^{40,41} the fracture initiation energy should be expected to increase. This is consistent with an increase in fracture initiation energy shown in Table III and the load–displacement curves shown in Figure 4. Since microvoids are nucleated at the site of organoclay platelets, it is expected that the impact strength is increased with increasing organoclay dispersion, i.e., when the compatibilizer is added. These results are similar to that of Misra et al.³⁷ for organoclay-reinforced polypropylene nanocomposites but not for

organoclay-reinforced polyethylene.²⁷ In the latter case, it is likely that the number of sites for microvoids formation and plastic deformation was much less than in our case, hence the lower impact strength. This difference arises because of the difference in molecular weight of the HDPE employed.

It has been shown that HDPE–organoclay composites with improved modulus and notched impact strength can be prepared. It may be postulated that there are various factors contributing to these improved properties. To obtain an increase in modulus and yield strength, good organoclay dispersion and good adhesion between the organoclay platelets and the matrix must be obtained. To obtain an increase in impact strength, the HDPE matrix should have a relatively low molecular weight, i.e., injection molding grade. Under these circumstances, the presence of organoclay will result in increased yield strength. It will also influence the deformation behavior of the matrix by suppressing strain hardening during tensile testing. These situations are thought to be important for the toughening effect of organoclay.

CONCLUSIONS

HDPE-organoclay composites with different organoclay contents and different degrees of organoclay dispersion were prepared. Composites with improved modulus, yield strength, and notched impact strength were obtained. Various factors contributed to these improvements. For an increase in modulus and yield strength, a high degree of organoclay dispersion, good adhesion between organoclay platelets and the matrix, and the orientation of organoclay platelets are the key factors. For an increase in notched impact strength, the matrix should have an appropriately low molecular weight so that the presence of organoclay will alter the deformation behavior by suppressing strain hardening during tensile deformation. Under impact conditions, the good adhesion between organoclay and the matrix and the high yield strength of the composite prolong failure deformation. This increased storage energy is released through microvoid formation and plastic deformation around each organoclay platelet. The composites will have higher impact strength.

The authors thank P. Kittikhun, Naresuan University, for SEM works.

References

- Brydson, J. A. *Plastics Materials*, 7th ed.; Butterworth-Heinemann: Guildford, 1999.
- Baker, R. A.; Koller, L. L.; Kummer, P. E. In *Handbook of Filler for Plastics*, 2nd ed.; Katz, H. S.; Milevski, J. V., Eds.; Van Nostrand Reinhold: New York, 1987; Chapter 6, p 119.
- Chan, C. M.; Wu, J.; Li, J. X.; Cheung, Y. K. *Polymer* 2002, 43, 2981.
- Krishnamoorti, R.; Vaia, R. A., Eds. *Polymer Nanocomposites: Synthesis, Characterization, and Modelling*; ACS: Washington, 2002.
- Kojima, Y.; Usuki, A.; Kawasumi, M.; Okada, A.; Kurauchi, T.; Kamigaito, O. *J Polym Sci Part A: Polym Chem* 1993, 31, 1755.
- Liu, L. M.; Qi, Z. N.; Zhu, X. G. *J Appl Polym Sci* 1999, 71, 1133.
- Zhao, C.; Feng, M.; Gong, F.; Qin, H.; Yang, M. *J Appl Polym Sci* 2004, 93, 676.
- Gopakumar, T. G.; Lee, J. A.; Kontopoulou, M.; Parent, J. S. *Polymer* 2002, 43, 5483.
- Zhao, C.; Qin, H.; Gong, F.; Feng, M.; Zhang, S.; Yang, M. *Polym Degrad Stab* 2005, 87, 183.
- Osman, M. A.; Rupp, J. E. P.; Suter, U. W. *Polymer* 2005, 46, 1653.
- Bartczak, Z.; Argon, A. S.; Cohen, R. E.; Weinberg, M. *Polymer* 1999, 40, 2347.
- Pukanszky, B. In *Polypropylene: Structure, Blends and Composites*; Karger-Kocsis, J., Ed.; Chapman and Hall: London, 1995; Vol. 3, p 1.
- Hoffmann, H.; Grellmann, W.; Zilvar, V. In *Polymer Composites*; Sedlacek, B., Ed.; Walter de Gruyter & Co.: New York, 1986, p 233.
- Badran, B. M.; Galeski, A.; Kryszewski, M. *J Appl Polym Sci* 1982, 27, 3669.
- Fu, Q.; Wang, G. *Polym Eng Sci* 1992, 32, 94.
- Fu, Q.; Wang, G.; Shen, J. *J Appl Polym Sci* 1993, 49, 673.
- Fu, Q.; Wang, G. *J Appl Polym Sci* 1993, 49, 1985.
- Fu, Q.; Wang, G. *Polym Int* 1993, 30, 309.
- Wang, Y.; Lu, J.; Wang, G. *J Appl Polym Sci* 1997, 64, 1275.
- Wu, S. *J Appl Polym Sci* 1988, 35, 549.
- Wu, S. *Polymer* 1985, 26, 1855.
- Bartczak, Z.; Argon, A. S.; Cohen, R. E.; Kowalewski, T. *Polymer* 1999, 40, 2367.
- Tanniru, M.; Misra, R. D. K. *Mater Sci Eng A* 2005, 405, 178.
- Nathani, H.; Dasari, A.; Misra, R. D. K. *Acta Mater* 2004, 52, 3217.
- Misra, R. D. K.; Nathani, H.; Dasari, A. *Mater Sci Eng A* 2004, 386, 175.
- Hadal, R. S.; Misra, R. D. K. *Mater Sci Eng A* 2004, 374, 374.
- Tanniru, M.; Yuan, Q.; Misra, R. D. K. *Polymer* 2006, 47, 2133.
- Wunderlich, B. *Macromolecular Physics*; Academic Press: New York, 1980; Vol. 3.
- Olley, R. H.; Bassett, D. C. *Polym Commun* 1982, 23, 1707.
- Peacock, A. J. *Handbook of Polyethylene: Structures, Properties, and Applications*; Marcel Dekker: New York, 2000.
- Osman, M. A.; Atallah, A. *Macromol Rapid Commun* 2004, 25, 1540.
- Chen, B.; Bowden, A. A.; Greenwell, H. C.; Boulet, P.; Covey, P. V.; Whiting, A.; Evans, J. R. G. *J Polym Sci Part B: Polym Phys* 2005, 43, 1785.
- Wu, D.; Wang, X.; Song, Y.; Jin, R. *J Appl Polym Sci* 2004, 92, 2714.
- Ravi, S.; Takahashi, K. *Polym Eng Sci* 2002, 42, 2146.
- Clois, E. P.; Gary, W. B. *Curr Opin Solid State Mater Sci* 2006, 10, 73.
- Yuan, Q.; Misra, R. D. K. *Polymer* 2006, 47, 4421.
- Deshmane, C.; Yuan, Q.; Misra, R. D. K. *Mater Sci Eng A* 2007, 460, 277.
- Tanniru, M.; Misra, R. D. K. *Mater Sci Eng A* 2006, 424, 53.
- UTHSCSA. ImageTool program; University of Texas Health Science Center, San Antonio, Texas. Available at: <http://ddsdx.uthscsa.edu/dig/itdesc.html>.
- Haworth, B.; Raymond, C. L.; Sutherland, I. *Polym Eng Sci* 2001, 41, 1345.
- Suwanprateep, J. *Polym Plast Technol Eng* 2000, 39, 83.